Accuracy and reliability of mandibular digital model registration with use of the mucogingival junction as the reference

Marcos Ioshida, DDS,[a] Brian Andres Muñoz, DDS,[b] Hector Rios, DDS, PhD,[c] Lucia Cevidanes, DDS, MS, PhD,[d] Juan Fernando Aristizabal, DDS,[e] Diego Rey, DDS,[f] Hera Kim-Berman, DDS, MMSc,[g] Marilia Yatabe, DDS, MS, PhD,[h] Erika Benavides, DDS, PhD,[i] Maria Antonia Alvarez, DDS,[j] Sarah Volk, BS,[k] and Antonio C. Ruellas, DDS, MS, PhD[l,m]

Objective. The aim of the study was to validate a method of mandibular digital model (DM) registration, acquired from an intraoral scanner, compared with high-resolution voxel-based cone beam computed tomography (CBCT) registration with use of the mucogingival junction as the reference.

Study Design. Pre- and post-treatment CBCT and DM images from 12 adults were randomly selected from an initial sample of 40 patients who had undergone orthodontic treatment. The DM registration was performed in 6 steps: (1) construction of 3-dimensional (3-D) volumetric label maps of CBCT scans, (2) voxel-based registration of CBCT scans, (3) prelabeling of CBCT images, (4) approximation and registration of DM models to the corresponding CBCT models, (5) mucogingival-junction registration of pretreatment and post-treatment DM images, and (6) measurements. The Mann-Whitney U test was used to calculate the significance of differences between the CBCT and DM registrations. The intraclass correlation coefficient (ICC) was performed to assess reproducibility of the registration method.

Results. When registered CBCT models and registered DM models were compared, no statistically significant differences in the measurements were found (right−left $P = .267$; anterior−posterior $P = .238$; superior−inferior $P = .384$; and 3-D $P = .076$). ICC showed excellent intra- and inter-rater correlation (ICC > 0.90).

Conclusions. The method of DM registration of the mandible with use of the mucogingival junction as the reference is accurate, reliable, and reproducible. (Oral Surg Oral Med Oral Pathol Oral Radiol 2019;127:351−360)

Three-dimensional intraoral scanning has been widely used for clinical and research purposes.[1] The sensor tip scans the teeth and soft tissue surfaces and converts the acquired optical data into a 3-dimensional (3-D) digital model (DM).[2] DMs have several advantages compared with stone casts: no need for physical storage of dental models, more efficient clinical workflow, improved patient acceptance, and reduced chair time.[3] In addition, the accuracy and quality of DMs

Statement of Clinical Relevance

Intraoral scanners in dentistry allow clinicians to superimpose digital images to accurately and reliably evaluate dental and soft tissue changes without exposing patients to ionizing radiation.

Funding support was provided by the Osteology Foundation [grant number 15-097 (HFR).

[a]Research Fellow, Department of Orthodontics and Pediatric Dentistry, School of Dentistry, University of Michigan, Ann Arbor, MI, USA.
[b]Resident of orthodontics, Valle University, Cali, Colombia.
[c]Adjunct Clinical Associate Professor, Department of Periodontics and Oral Medicine, School of Dentistry, University of Michigan, Ann Arbor, MI, USA.
[d]Associate Professor, Department of Orthodontics and Pediatric Dentistry, School of Dentistry, University of Michigan, Ann Arbor, MI, USA.
[e]Associate Professor and Head, Department of Orthodontics, Universidad del Valle, Colombia.
[f]Associate Professor and Head, Department of Orthodontics, CES University, Medellin, Colombia.
[g]Program Director and Clinical Assistant Professor, Department of Orthodontics and Pediatric Dentistry, School of Dentistry, University of Michigan, Ann Arbor, MI, USA.
[h]Craniofacial Fellow, Department of Orthodontics and Pediatric Dentistry, School of Dentistry, University of Michigan, Ann Arbor, MI, USA.
[i]Clinical Associate Professor, Division of Oral Pathology/Medicine/Radiology, Department of Periodontics and Oral Medicine, School of Dentistry, University of Michigan, Ann Arbor, MI, USA.
[j]Resident of orthodontics, CES University, Medellin, Colombia.
[k]Clinical Research Coordinator, Internal Medicine, Division of Gastroenterology, Michigan Medicine, University of Michigan, Ann Arbor, MI, USA.
[l]Associate Professor, Department of Orthodontics and Pediatric Dentistry, School of Dentistry, University of Michigan, Ann Arbor, MI, USA.
[m]Associate Professor, Department of Orthodontics and Pediatric Dentistry, School of Dentistry, Federal University of Rio de Janeiro, Rio de Janeiro, RJ, Brazil.

Received for publication Apr 30, 2018; returned for revision Oct 3, 2018; accepted for publication Oct 6, 2018.

© 2018 Elsevier Inc. All rights reserved.

2212-4403/$-see front matter
https://doi.org/10.1016/j.oooo.2018.10.003

have been considered adequate for clinical purposes compared with standard dental casts.[2,4,5]

Cone beam computed tomography (CBCT) has been used as a substitute for conventional radiography for multiple clinical applications.[1,6] In the last decade, CBCT images with a small field of view (FOV) have been used for head and neck applications according to the ALARA (As Low As Reasonably Achievable) principle of minimizing radiation dosage. The main advantages of CBCT are its capability to produce 3-D digital imaging of dental and craniofacial structures and to visualize root and bone structures without the distortions that can be present on conventional radiographs.[2] However, the low-radiation-dose CBCT images that are often used in clinical dentistry do not show the dental anatomy, interocclusal relationship, and periodontal soft-tissue in sufficient detail. Furthermore, repeated exposure to low-radiation-dose CBCT can still lead to cumulative radiation effects.[7]

To assess dental changes after treatment, studies have used superimposition of different time points of DMs without using CBCT.[3,8] The greatest challenge in registering DMs is finding a stable structure to use as a reference for superimposition.[2,3,8-11] Studies using mini-screws or implants for registration landmarks have proven to be accurate, but this method cannot be considered for all patients.[10,11] Palatal rugae have been used as a stable structure of reference, but they are only useful for superimposition of the maxilla.[2,3,8] The following anatomic areas have also been suggested for mandibular registration: (1) bilateral lingual alveolar surfaces of premolars and molars, (2) lingual alveolar surface of the entire dentition, (3) bilateral buccal and lingual alveolar surfaces of the premolar and molar areas, and (4) bilateral mandibular tori. However, none of these structures has been considered stable.[12] To date, there is little information on reliable and reproducible references for mandibular DM registration. This study investigated the use of the mucogingival junction of the mandibular arch as an anatomic reference because it remains stable even after tooth movement.[13-15]

The purpose of this study was to validate a method of mandibular DM registration, acquired from an intraoral scanner, to evaluate dental movements and compare the results with the previously validated method of voxel-based mandibular registration acquired by using CBCT with use of the mandibular mucogingival junction as the reference.

MATERIALS AND METHODS

The study was approved by the institutional review board (HUM00133283) of the University of Michigan. Twelve patients were randomly selected from a sample of 40 adult patients who had undergone orthodontic treatment for mandibular anterior crowding. None of the patients had any signs of an inflammatory response in the periodontal soft tissue. The data consisted of CBCT scans and DMs at 2 different time points: pretreatment (T1) and post-treatment (T2). Pretreatment data were collected before orthodontic appliance placement and post-treatment data were acquired after 48 weeks of orthodontic treatment. The CBCT scans were obtained by using Veraviewepocs 3-D R100 (J Morita Corp., Tokyo, Japan) according to the acquisition protocol with the following parameters: FOV 100×80 mm; 0.16 mm^3 voxel size; 90 kVp; 3 to 5 mA; and 9.3 seconds.

DMs of the mandibular arch were acquired with the TRIOS 3-D intraoral scanner (3 Shape, Copenhagen, Denmark; software version: TRIOS 1.3.4.5). The TRIOS intraoral scanner utilizes "ultrafast optical sectioning"[16] and confocal microscopy to generate 3-D images from multiple 2-dimensional images with accuracy of 6.9 ± 0.9 μm. All scans were obtained, according to the manufacturer's instructions, by 1 trained operator. Two open-source software products, ITK-snap, version 3.6 (www.itksnap.org)[17,18] and 3-D SlicerCMF, version 4.0 (https://sites.google.com/a/umich.edu/dentistry-image-computing/Download),[19] were used assess the data in 3-D, as described below.

1 *Construction of the 3-D volumetric label maps of CBCT scans (segmentation):* 3-D volumetric label maps (segmentation) at T1 and T2 were created by segmenting all CBCT scans by using ITK Snap software.[17,18]
2 *Voxel-based CBCT registration:* Rami, teeth, and alveolar bone were removed from the mandibular segmentation, keeping the mandibular body as a region of reference (mask).[20] Using a nongrowing registration module on SlicerCMF,[19] the mask indicated to the software which areas it should register the voxels of T2 CBCT scans in relation to T1 (Figure 1).
3 *Prelabeling:* Ten 3-D dots were placed on the distal and mesial incisal edges of the incisors and canine cusp tip by changing the color of the segmentation, without modifying the dental anatomy. These 3-D dots help standardize the landmark placement used to measure and quantify the tooth movement at T1 and T2[21] (Figure 2). After CBCT registration and prelabeling, the T1 and T2 mandibular 3-D surface models (.stl file format) were constructed as CBCT models on SlicerCMF.[19]
4 *Approximation and registration of DMs to the corresponding CBCT models on SlicerCMF:*
   a Approximation—to approximate the T1 DM to T1 CBCT model, landmarks were placed over the mesiobuccal cusp of the second molar, buccal

cusp of the second premolar, and canine tip on the left and right sides of the CBCT models and DMs (Figure 3). The SlicerCMF software computed and approximated the models by using the landmarks, creating a new file as "approximated DM."

b Registration—one landmark was placed at the center of the buccal surface of all teeth in both the CBCT model and the approximated DM at T1. The SlicerCMF software automatically computes and registers the models, creating the new registered DM file as "T1−DM/CBCT" (Figure 4).

The same procedure was repeated to complete the approximation and registration at T2 to create the new registered file as "T2−DM/CBCT."

1 *Mucogingival-junction registration of T2 DM over T1 DM:* The files "T2−DM/CBCT" were then registered over "T1−DM/CBCT" by placing landmarks on the mucogingival junction between molars, between the molar and he premolar, between premolars, between the premolar and the canine, and between the canine and the lateral incisors on both the right and left sides. The SlicerCMF software created a new registered DM file (which had the mucogingival junction as the reference) "DM/MJ" (Figure 5). An interactive data set is available.

2 *Measurements:* Measurements were performed between the T1 and T2 models registered in 2 different ways: (1) voxel-based registration (CBCT model)[20] and (2) landmark-based registration with use of the mucogingival junction as the reference (DM/MJ). Dental landmarks corresponding to those prelabeled (step 3) on the CBCT models (distal and mesial incisal edges of the incisors and canine cusp tips) were placed on the surface of the DM/MJ models (Figure 6) by using the "Quantification of 3-D Components [Q3-DC]" tool in SlicerCMF.[19] This tool allows users to compute the 3-D distance landmarks, as well as the distances along each of the axes in the 3-D space: right−left (RL), anterior−posterior (AP), superior−inferior (SI) components, and 3-D distances. The distances between T1 and T2 voxel-based registrations were compared with the distances

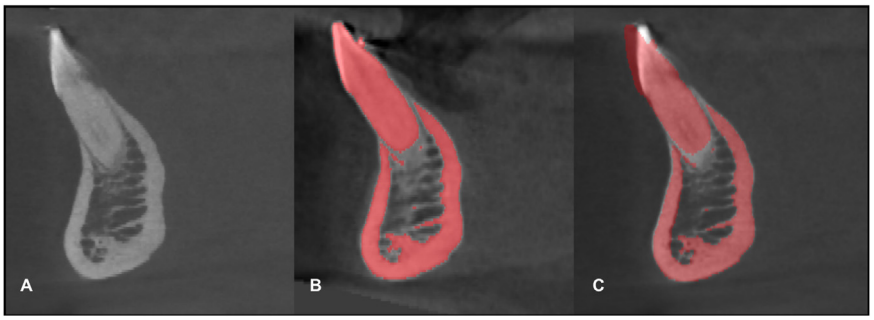

Fig. 1. Regional voxel-based registration. T1 cone beam computed tomography (CBCT) (**A,** pretreatment), T2 CBCT (**B,** post-treatment), and overlay of the T1 CBCT scan and T2 segmentation (**C,** difference after registration between T1 and T2). Note that the lower incisor in T2 shown in red has flared compared with the T1 CBCT scan.

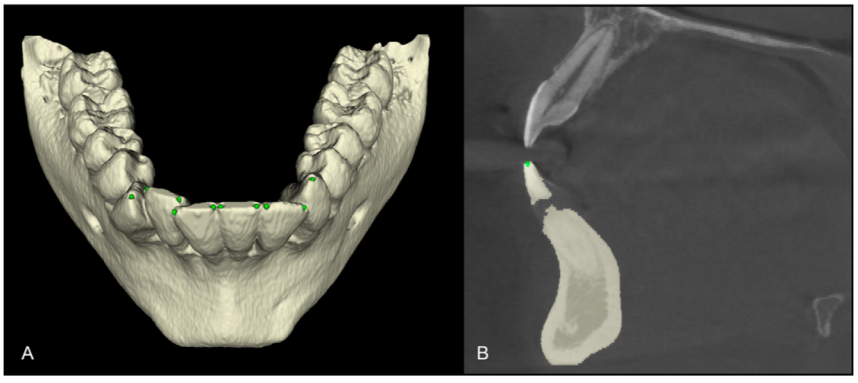

Fig. 2. Prelabeling in ITKsnap. **A,** Segmentation with 3-D dots. **B,** Sagittal view to guide the 3-dimensional (3-D) dot placement. Note: Coronal and axial views were also used to guide the 3-D dot placement.

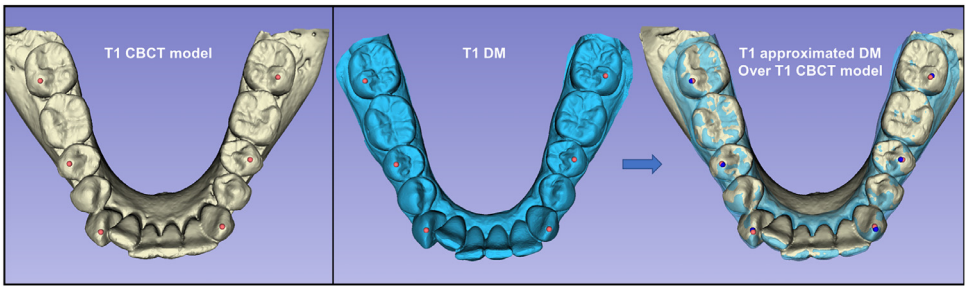

Fig. 3. Occlusal view of landmark-based approximation of pretreatment (T1) digital model (DM) over its corresponding cone beam computed tomography (CBCT) model. New file created as T1 "approximated DM." This step was also performed for the post-treatment (T2) models.

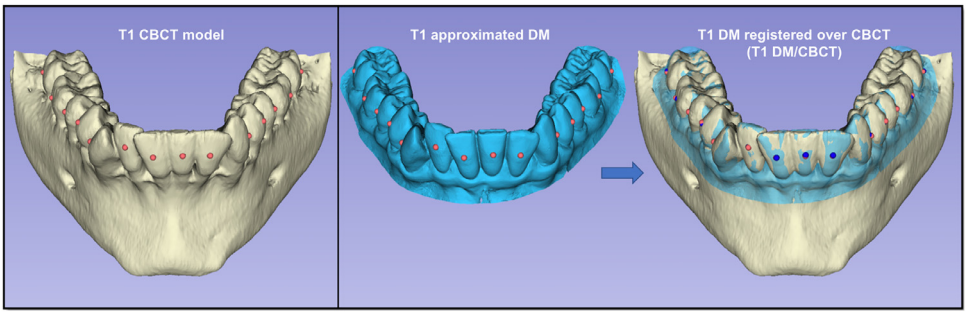

Fig. 4. Frontal view of landmark-based registration of pretreatment (T1) of the approximated digital model (DM) over its corresponding cone beam computed tomography (CBCT) model. New file created as "DM/CBCT." This step was also performed for the post-treatment (T2) models.

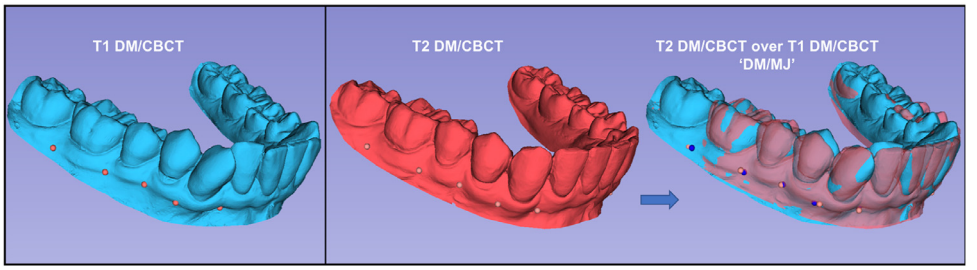

Fig. 5. Frontal view of landmark-based registration on the mucogingival junction of pretreatment (T1) and post-treatment (T2) digital model/cone beam computed tomography (DM/CBCT). New file created as "DM/MJ."

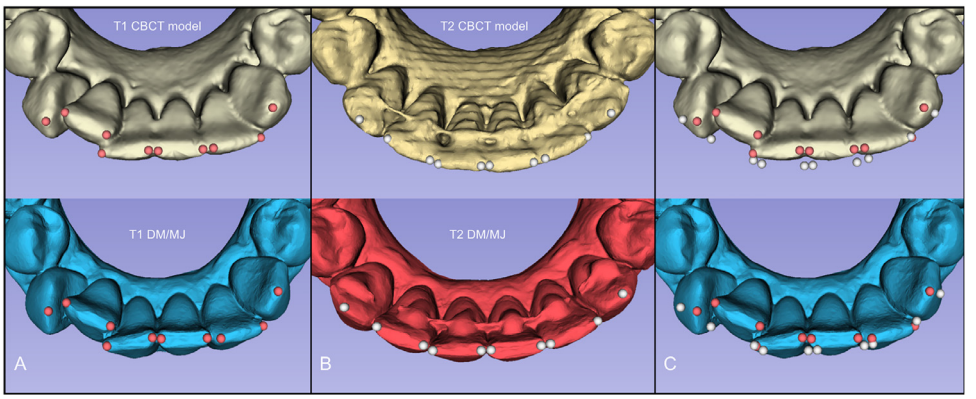

Fig. 6. Ten landmarks were placed on the canine cusp tips, and the mesial and distal incisal edges of the lower incisors are shown as red landmarks in T1 models **(A)** and as white landmarks in T2 models **(B)**. **C,** Differences in location between the T1 and T2 landmarks of the cone beam computed tomography (CBCT) and digital model (DM) measurements. Q3-DC was used to compute the distances between the T1 and T2 landmarks.

between the T1 and T2 registrations with use of the mucogingival junction as the reference (see Figure 6). (Video tutorials are available on YouTube on the Dental and Craniofacial Bionetwork for Image Analysis' [DCBIA][22] channel.)

To evaluate the intrarater reliability of the CBCT and DM methods, rater 1 (M.I., an implantologist) repeated the registration and measurements within an interval of 2 weeks. It was tested by using the intraclass correlation coefficient (ICC) based on a single rater ($k = 1$), using absolute agreement and the 2-way mixed-effects model at a 95% confidence interval. To determine the inter-rater reliability of the DM method, rater 2 (A.C.R., an orthodontist) registered and measured the same samples as those used by rater 1. The results between rater 1 and rater 2 were compared by using ICC based on a mean-rating ($k = 2$), consistency and 2-way random-effects model at 95% confidence interval. Bland-Altman plots were used to illustrate the level of agreement.

For accuracy, the Mann Whitney U test was used to compare the measurements from CBCT voxel-based registration with the measurements from DM landmark-based registration (significance established at $P = .05$). All statistical analyses were performed by using SPSS Statistics for Mac, version 24.0 (SPSS Inc., Chicago, IL).

RESULTS

Intrarater reliability

ICC results showed excellent agreement (above 0.90)[23] for measurements on both CBCT and DM registrations (Table I).

The Bland-Altman plot illustrates the high level of agreement of intrarater reliability (Figure 7).

Inter-rater reliability

When comparing the measurements from the DM registration method, ICC results showed excellent inter-rater agreement (above 0.90)[23] (Table II). The Bland-Altman plot illustrated a high level of inter-rater agreement (Figure 8).

CBCT versus DM

Dental measurements after DM registration showed no statistically significant difference compared with CBCT registration with regard to the RL, AP, SI, and 3-D components ($P > .05$) (Table III). A flowchart depicting the steps for the method of mandibular DM registration is provided in Figure 9.

DISCUSSION

Complete diagnostic records and thorough evaluation are necessary to plan any treatment and to determine treatment outcomes for clinical and, sometimes, legal purposes.[24] In daily clinical practice, DMs can be useful to record and quantify tooth movement, update the treatment plan, show treatment progress and outcomes, and even evaluate pre- and post-treatment periodontal biotype changes. Compared with traditional dental casts, DMs cost less (after initial acquisition), require less physical space for storage, and facilitate virtual integration and registration with other complementary digital records, such as CBCT scans.

Management of virtual models is more convenient, as these models allow for virtual treatment simulations in treatment planning, choice of therapies, and efficient digital workflow.[2,25] Another important advantage of DMs obtained by intraoral or indirect desktop scanners is that they provide a clear and fine contour of the attached gingiva, with reliable and reproducible information regarding the periodontal biotype.[26]

A method of mandibular DM registration has not been previously established in the literature. This is the

Table I. Intrarater agreement (first vs second measurements)*

		ICC intrarater agreement (rater 1)					
		First measurement vs second measurement			*95% confidence interval*		
	Component	*Mean difference 1 (SD)*	*Mean difference 2 (SD)*	*ICC*	*Lower bound*	*Upper bound*	*Reliability*
CBCT	RL	−0.038 (0.962)	−0.027 (0.963)	0.994	0.991	0.996	Excellent
	AP	1.224 (1.211)	1.225 (1.211)	0.996	0.994	0.997	Excellent
	SI	0.284 (0.989)	0.276 (0.977)	0.992	0.989	0.994	Excellent
	3-D	2.005 (0.953)	1.996 (0.959)	0.992	0.989	0.995	Excellent
DM	RL	−0.146 (0.866)	−0.175 (0.878)	0.974	0.963	0.982	Excellent
	AP	1.021 (1.173)	1.043 (1.203)	0.980	0.971	0.986	Excellent
	SI	0.279 (0.847)	0.347 (0.812)	0.929	0.898	0.950	Good- Excellent
	3-D	1.773 (0.909)	1.817 (0.893)	0.947	0.924	0.962	Excellent

*Mean difference shown in millimeters.*3-D,* 3-dimensional; *AP,* anterior−posterior; *CBCT,* cone beam computed tomography; *DM,* digital model; *ICC,* intraclass correlation coefficient; *RL,* right−left; *SD,* standard deviation; *SI,* superior−inferior.

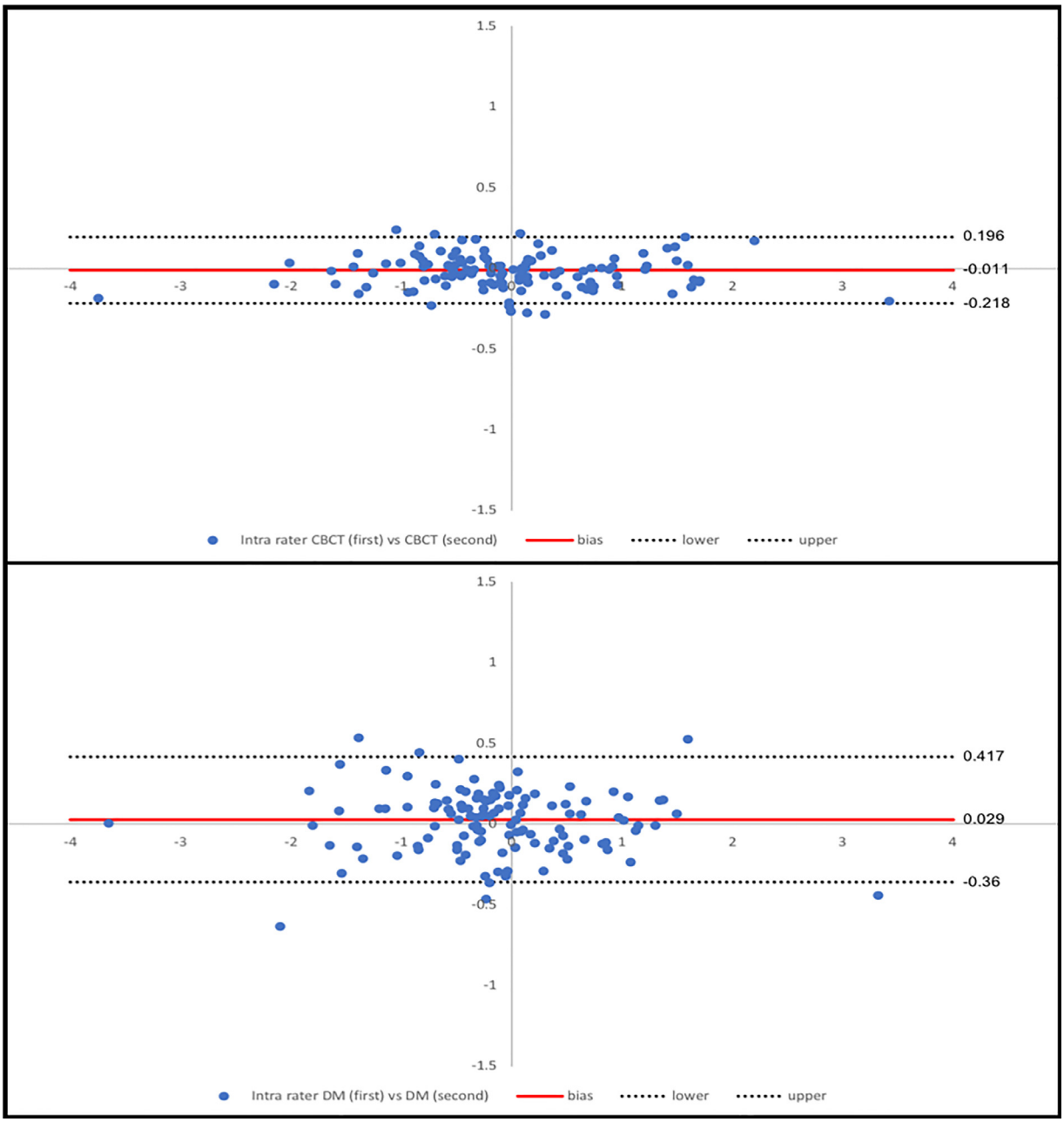

Fig. 7. Bland-Altman plot of intrarater agreement of **(A)** cone beam computed tomography (CBCT) and **(B)** digital model (DM) measurements. Each circle represents the difference between the first and second measurements. The red line indicates the mean difference, and the dashed line shows the 95% limits of agreement (LOA).

first study to validate such a method, with images acquired from an intraoral scanner, and compare the results with the previously validated method of voxel-based mandibular registration acquired via CBCT. The findings of this study showed significant improvement in accuracy compared with the region of interest registration used by Kiyong et al.[12]

Additionally, the open-source software that is available for 3-D analysis of CBCT images can now be used for superimposition of soft and hard tissue structures, as well as for longitudinal evaluation of tissue changes after therapy using DMs.[27] This study proposed superimposition of DMs with use of the mucogingival junction as an anatomic reference in the mandible because this anatomic area remains stable even after tooth movement and does not change significantly.[13-15]

The study findings of excellent intrarater and inter-rater agreement, with ICC > 0.90 in all

Table II. Inter-rater agreement between rater 1 and rater 2*

		ICC inter-rater agreement					
	Component	*Rater 1*	*Rater 2*	*ICC*	*95% confidence interval*		*Reliability*
		Mean difference (SD)	*Mean difference (SD)*		*Lower bound*	*Upper bound*	
DM	RL	−0.146 (0.866)	−0.119 (0.906)	0.988	0.983	0.992	Excellent
	AP	1.021 (1.173)	1.014 (1.189)	0.994	0.992	0.996	Excellent
	SI	0.279 (0.847)	0.261 (0.748)	0.956	0.937	0.969	Excellent
	3-D	1.773 (0.909)	1.754 (0.902)	0.979	0.970	0.985	Excellent

*Mean difference shown in millimeters.*3-D,* 3-dimensional; *AP,* anterior−posterior; *CBCT,* cone beam computed tomography; *DM,* digital model; *ICC,* intraclass correlation coefficient; *RL,* right−left; *SD,* standard deviation; *SI,* superior−inferior.

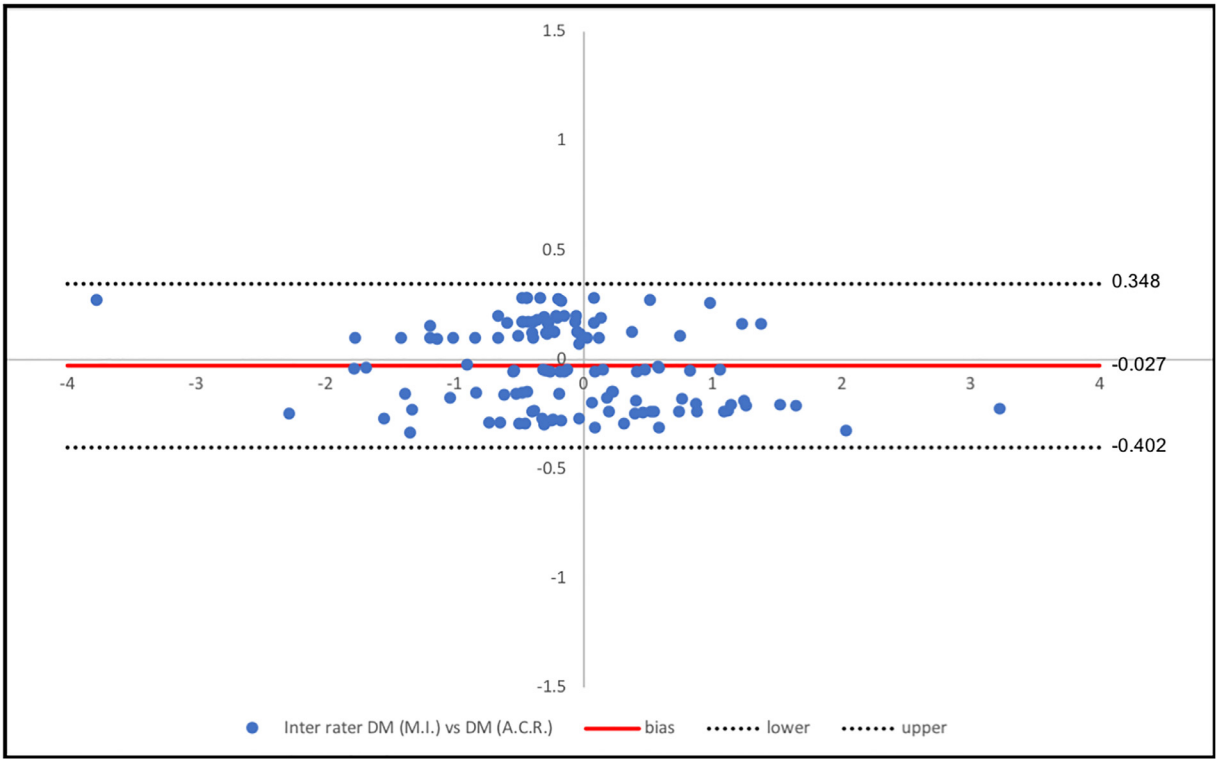

Fig. 8. Bland-Altman plot of inter-rater agreement of digital model (DM; rater 1) versus DM (rater 2). Each circle represents the difference between the measurements from rater 1 and rater 2. The red line indicates the mean difference, and the dashed line shows the 95% limits of agreement (LOA).

coordinates, indicate that DMs can be reliably registered and superimposed at different timepoints and by different raters. Additionally, because this study demonstrated that there was no significant difference in the measurements of anterior teeth between CBCT models and DM superimpositions ($P > .05$), the registration of the initial DM to an initial CBCT model can be used to compare and follow up the associated clinical outcomes by using DMs without further radiation exposure with a post-treatment CBCT.

On the basis of the results of this study, this method of registration with use of intraoral scanners and DMs

Table III. Mann-Whitney U Test showed that there was no statistical significance between CBCT models and DM measurements ($P > .05$)*

	Mann-Whitney U test (rater 1)		
	CBCT models *Mean difference (SD)*	*DM* *Mean difference (SD)*	*P value*
RL	−0.027 (0.963)	−0.175 (0.878)	.262
AP	1.225 (1.211)	1.043 (1.203)	.238
SI	0.276 (0.977)	0.347 (0.812)	.384
3-D	1.996 (0.959)	1.817 (0.893)	.076

*Mean difference shown in millimeters.*3-D,* 3-dimensional; *AP,* anterior−posterior; *CBCT,* cone beam computed tomography; *DM,* digital model; *ICC,* intraclass correlation coefficient; *RL,* right−left; *SD,* standard deviation; *SI,* superior−inferior.

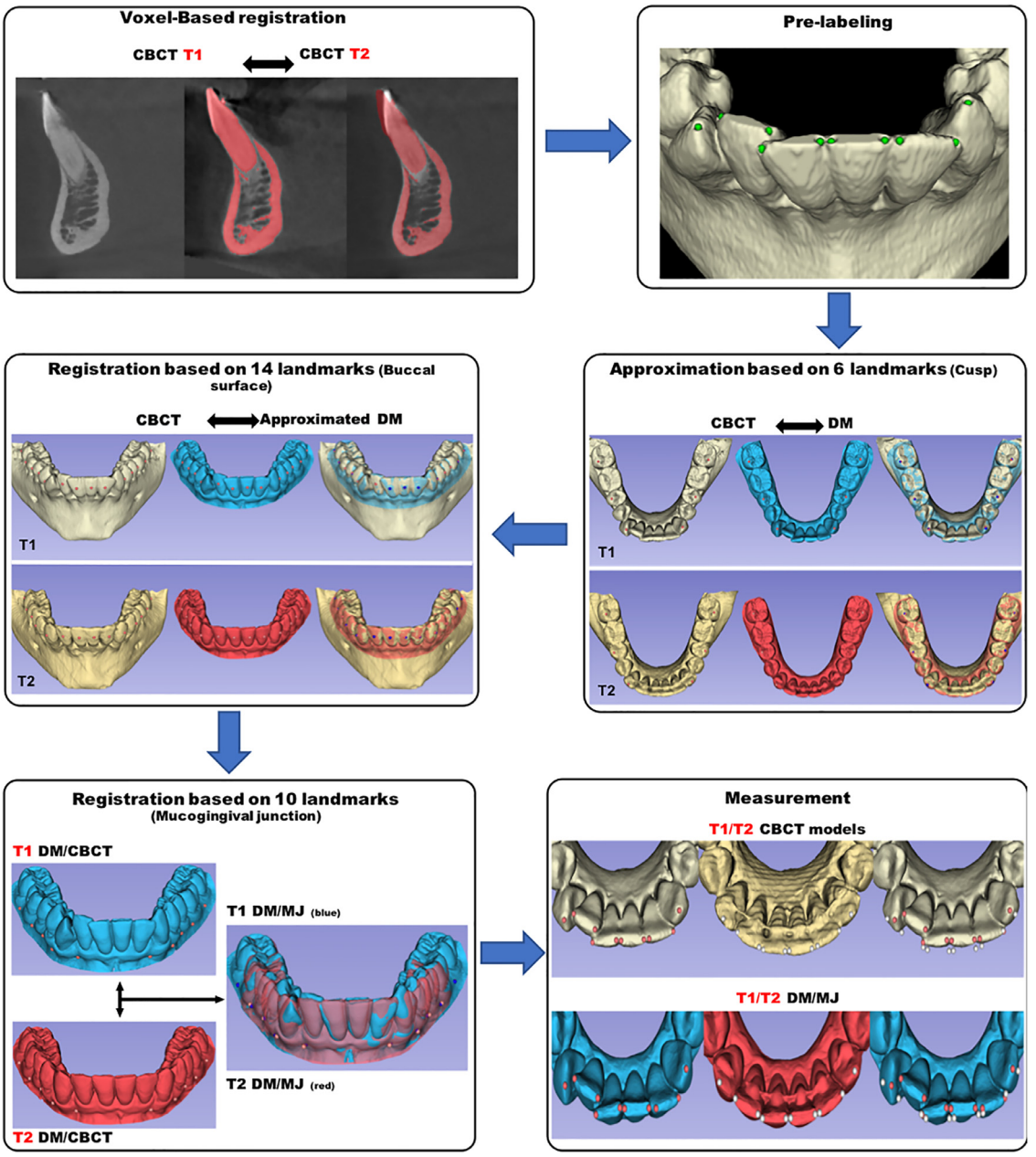

Fig. 9. Flowchart of the steps for the method of mandibular digital model (DM) registration.

may be applied to assess longitudinal changes in different fields of dentistry, including periodontics, implant dentistry, prosthodontics, oral surgery, and orthodontics. Furthermore, with DMs soft tissue information can be obtained, whereas it is not possible with CBCT, which only shows skeletal and dental components. As an example of potential clinical application, superimposition of the initial CBCT model with follow-up DMs at different time points of interest can now be used in future studies to evaluate gingival dimensional changes after soft tissue grafting or any xeno- or allograft alternative around teeth or implants. Because many gingival or periodontal problems often occur in patients with a thin biotype, accurate knowledge of the thickness and volume of the masticatory mucosa obtained from a combination of CBCT and DM superimpositions may help determine the appropriate treatment method and predict the outcomes of several surgical procedures.[26] Although the mucogingival line is a stable anatomic landmark that is not permanently altered by either orthodontics or surgery,[28,29] the validated methods used in this study may have greater errors if teeth have been moved out of the alveolar bone housing (i.e., when an alveolar bone dehiscence

is created) or if severe periodontal disease develops longitudinally.

The high levels of intrarater agreement and interrater agreement (see Tables I and II, respectively) for DMs are comparable with previous studies on registration that used CBCT examinations.[20,30] Therefore, it may be possible to use either CBCT or DM superimpositions to compare different treatment groups and treatment outcomes in future studies. The main limitations of this methodology might become evident if therapy includes a large amount of tooth movement (i.e., orthodontic expansion or a great amount of extrusion)[31] and signs of an inflammatory response in the gingival area.

This study validates the superimposition of 2 DMs; the methods in this study achieved similar results with superimposing only DMs and with superimposing CBCTs. Therefore, for the specific applications of dental changes, such superimposition of DMs may decrease the need for and risks of cumulative radiation exposure[32,33] because no CBCT scanning will be needed for future assessments. On the basis of our findings, it is possible to suggest that the DM registration with use of the mucogingival junction as the reference is accurate, reliable, and reproducible.

SUPPLEMENTARY MATERIALS

Supplementary material associated with this article can be found in the online version at doi:10.1016/j.oooo.2018.10.003.

REFERENCES

1. de Waard O, Baan F, Verhamme L, Breuning H, Kuijpers-Jagtman AM, Maal T. A novel method for fusion of intra-oral scans and cone-beam computed tomography scans for orthognathic surgery planning. *J Craniomaxillofac Surg*. 2016;44:160-166.
2. Kim J, Heo G, Lagravere MO. Accuracy of laser-scanned models compared to plaster models and cone-beam computed tomography. *Angle Orthod*. 2014;84:443-450.
3. Chen G, Chen S, Zhang XY, et al. Stable region for maxillary dental cast superimposition in adults, studied with the aid of stable miniscrews. *Orthod Craniofac Res*. 2011;14:70-79.
4. Anh JW, Park JM, Chun YS, Kim M, Kim M. A comparison of the precision of three-dimensional images acquired by 2 digital intraoral scanners: effects of tooth irregularity and scanning direction. *Korean J Orthod*. 2016;46:3-12.
5. Cho SH, Schaefer O, Thompson GA, Guentsch A. Comparison of accuracy and reproducibility of casts made by digital and conventional methods. *J Prosthet Dent*. 2015;113:310-315.
6. Jager F, Mah JK, Bumann A. Peridental bone changes after orthodontic tooth movement with fixed appliances: a cone-beam computed tomographic study. *Angle Orthod*. 2017;87:672-680.
7. Rangel FA, Maal TJ, Berge SJ, Kuijpers-Jagtman AM. Integration of digital dental casts in cone-beam computed tomography scans. *ISRN Dent*. 2012;2012:949086.
8. Gibelli D, De Angelis D, Pucciarelli V, et al. Application of 3-D models of palatal rugae to personal identification: hints at identification from 3-D-3-D superimposition techniques. *Int J Legal Med*. 2017.
9. Bjork A. Facial growth in man, studied with the aid of metallic implants. *Acta Odontol Scand*. 1955;13:9-34.
10. Parton AL, Duncan WJ, Oliveira ME, Key O, Farella M. Implant-based three-dimensional superimposition of the growing mandible in a rabbit model. *Eur J Orthod*. 2016;38:546-552.
11. Jang I, Tanaka M, Koga Y, et al. A novel method for the assessment of three-dimensional tooth movement during orthodontic treatment. *Angle Orthod*. 2009;79:447-453.
12. An K, Jang I, Choi DS, Jost-Brinkmann PG, Cha BK. Identification of a stable reference area for superimposing mandibular digital models. *J Orofac Orthop*. 2015;76:508-519.
13. Batenhorst KF, Bowers GM, Williams Jr, JE. Tissue changes resulting from facial tipping and extrusion of incisors in monkeys. *J Periodontol*. 1974;45:660-668.
14. Kajiyama K, Murakami T, Yokota S. Gingival reactions after experimentally induced extrusion of the upper incisors in monkeys. *Am J Orthodont Dentofac Orthoped*. 1993;104:36-47.
15. Brindis MA, Block MS. Orthodontic tooth extrusion to enhance soft tissue implant esthetics. *J Oral Maxillofac Surg*. 2009;67:49-59.
16. 3 Shape. Available at: https://www.3shape.com/en/knowledge-center/news-and-press/press-releases/2013/3 shape-launches-trios-color#. Accessed 16 March 2018.
17. Yushkevich PA, Gerig G. ITK-SNAP: an intractive medical image segmentation tool to meet the need for expert-guided segmentation of complex medical images. *IEEE Pulse*. 2017;8:54-57.
18. Yushkevich PA, Piven J, Hazlett HC, et al. User-guided 3-D active contour segmentation of anatomic structures: significantly improved efficiency and reliability. *Neuroimage*. 2006;31:1116-1128.
19. SlicerCMF. Available at: https://sites.google.com/a/umich.edu/dentistry-image-computing/Download. Accessed 16 March 2018.
20. Ruellas AC, Yatabe MS, Souki BQ, et al. 3-D mandibular superimposition: comparison of regions of reference for voxel-based registration. *PLoS One*. 2016;11:e0157625.
21. Ruellas AC, Huanca Ghislanzoni LT, Gomes MR, et al. Comparison and reproducibility of 2 regions of reference for maxillary regional registration with cone-beam computed tomography. *Am J Orthodont Dentofac Orthoped*. 2016;149:533-542.
22. DCBIA. Video Tutorials November 14, 2017. Available at: https://www.youtube.com/user/DCBIA. Accessed 16 March 2018.
23. Koo TK, Li MY. A guideline of selecting and reporting intraclass correlation coefficients for reliability research. *J Chiropr Med*. 2016;15:155-163.
24. Abdelkarim A, Jerrold L. Orthodontic chart documentation. *Am J Orthodont Dentofac Orthoped*. 2017;152:126-130.
25. Mangano F, Gandolfi A, Luongo G, Logozzo S. Intraoral scanners in dentistry: a review of the current literature. *BMC Oral Health*. 2017;17:149.
26. Yan S, Shi SG, Niu ZY, Pei ZH, Shi SM, Mu C. Soft tissue image reconstruction using cone-beam computed tomography combined with laser scanning: a novel method to evaluate the masticatory mucosa. *Oral Surg Oral Med Oral Pathol Oral Radiol*. 2014;118:725-731.

27. Fedorov A, Beichel R, Kalpathy-Cramer J, et al. 3-D Slicer as an image computing platform for the Quantitative Imaging Network. *Magn Reson Imaging*. 2012;30:1323-1341.
28. Anjcamo A, Bergenholtz A, Hugoson A, Ainamo J. Location of the mucogingival junction 18 years after apically repositioned flap surgery. *J Clin Periodontol*. 1992;19:49-52.
29. Wennstrom JL. Mucogingival considerations in orthodontic treatment. *Semin Orthod*. 1996;2:46-54.
30. Ghoneima A, Cho H, Farouk K, Kula K. Accuracy and reliability of landmark-based, surface-based and voxel-based 3-D cone-beam computed tomography superimposition methods. *Orthod Craniofac Res*. 2017;20:227-236.
31. Pikdoken L, Erkan M, Usumez S. Gingival response to mandibular incisor extrusion. *Am J Orthodont Dentofac Orthoped*. 2009;135(432):e431-e436. discussion e432-e433.
32. Fazel R, Krumholz HM, Wang Y, et al. Exposure to low-dose ionizing radiation from medical imaging procedures. *New England Journal of Medicine*. 2009;361:849-857.
33. Council NR. Committee to Assess Health Risks from Exposure to Low Levels of Ionizing Radiation, Health Risks from Exposure to Low Levels of Ionizing Radiation: BEIR VII Phase 2: Washington, DC: National Academies Press; 2006.

Reprint requests:

Marcos Ioshida
1011 North University Avenue
Ann Arbor
MI 48109
USA
Mioshida@umich.edu